HNPS Advances in Nuclear Physics
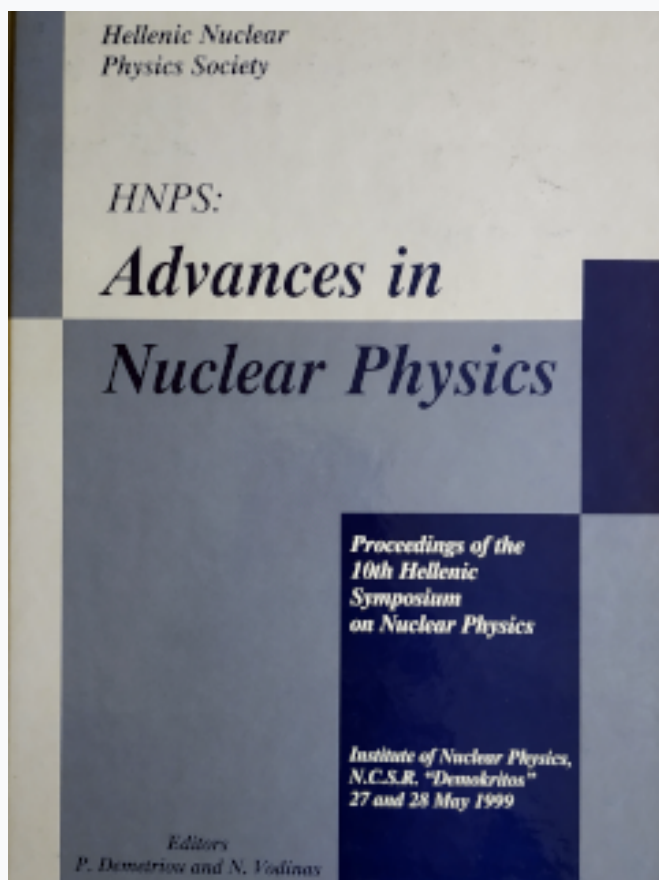
HNPS1999

Determination of Sulfur and Copper Profile with nuclear reactions

S. Kossionides, G. Kaliambakos, R. Vlastou, C. T. Papadopoulos

Determination of Sulfur and Copper Profile
with nuclear reactions

S. Kossionides[a], G. Kaliambakos[a], R. Vlastou[b]
and C.T. Papadopoulos[b]

[a] *Institute of Nuclear Physics, N.C.S.R. "Demokritos", GR-153 10 Aghia
Paraskevi, Athens, Greece*

[b] *Department of Physics, National Technical University of Athens, GR-157 80
Zografou, Athens, Greece*

Abstract

The concentration and depth profile of Cu and S in patinna samples have been de-
ternined by using Nuclear Reaction Analysis (NRA) and Rutherford Backscattering
Spectroscopy (RBS). For the NRA the differential cross section was mesaured for
the 1327 keV γ-ray deexciting the third excited state to the ground state of ^{63}Cu
through the reaction ^{63}Cu(p,p'γ), as well as, for the 2230 keV γ-ray deexciting the
first excited state to the ground state through the resonant reaction ^{32}S(p,p'γ). The
mesaurements of both excitation functions were performed in the energy range 3.0
- 3.7 MeV in 20 keV steps and at an angle of 125°.

1   Introduction

Copper and bronze artifacts, exhibited in public places (e.g. statues), form an
essential part of the European cultural heritage. The composition of patinna on
these artifacts is crucial for their preservation. Patinna consists of a combina-
tion of copper sulfate salts (such as brochandite $CuSO_4 3[Cu(OH)_2]$, antlerite
$CuSO_4 2[Cu(OH)_2]$, etc.). In the frame of a European Collaboration artificial
patinna samples were prepared and examined with various methods. The re-
actions ^{63}Cu(p,p'γ) and ^{32}S(p,p'γ) were used to obtain information on the
distribution of the two elements and hence on the composition of the patinna
layer. These nuclear reactions have also been used in the literature [1], [2] but
either the targets were gaseous or the energy range was different. During the
course of this work, it was attempted to use the data of [3] for the absolute
value of the sulfur cross section, as well as the data of [4] for the angular
distributions on the reaction resonances. It was found that the data from [3]

1

were taken with the Ge-Li detector placed at 90°, while our experimental data were taken at 125°, so we decided to remeasure the cross section of sulfur at that angle. In the same experiment we also measured the cross section of copper to confirm the data of the literature [5]. We report here on the measurements of the relevant cross sections and present several examples of their use for patinna analysis. Additional informations were obtained by using the RBS method for the depth profile of the heavier elements of the samples.

2   Experimental measurements

The patinna samples were obtained by courtesy of Prof. P. Missailides from Thessaloniki University. The experimental measurements that have been made concern irradiation of patinna samples with protons of energy 1.5 MeV for RBS measurements with a Si surface barrier detector placed at 160° with respect to the axis beam. Also protons of 3.375 - 3.700 MeV were used for (p,p'γ) measurements with the Ge-Li detector placed at 125°. With the same detector geometry, the cross sections for the (p,p'γ) reaction on Cu and S were also measured. To this purpose samples of pure copper and CdS respectively were irradiated with protons of energy 3.0 - 3.7 MeV with an energy step of 20 keV. The proton beam used for the irradiation was supplied by the Tandem T11/25 accelerator of the NRCPS "Demokritos" (figure 1), while data aquisition and control hardware were driven by a personal computer with the use of the appropriate software.

The incoming protons pass a $10\mu g/cm^2$ C-foil, on which a thin gold layer of thickness 8,7±0,4 $\mu gr/cm^2$ was evaporated. The thickness of the Au-layer was determined with an XRF measurement. The foil was placed on the beam-target line and after passing through it, the protons fall on the target without substantial loss of energy or angular spread. The protons scattered off the foil, were detected by a Si detector, placed at an angle of 37° with respect to the beam. From the measured yield we calculated the total charge that falls on the target by using the cross section for Rutherford scattering of protons on Au. The relation we used for the calculation of charge is

$$A = \sigma \, \Omega \, I \, N \, \tau \tag{1}$$

where A is the yield in number of counts; σ is the Rutherford cross section for Au, which is given by $(Z_1 Z_2 e^2/4E)sin(\theta/2)^{-4} cm^2$ (θ is the angle of scattering in the lab system); Ω is the solid angle of the detector, which was 0.9 msr for the geometrical setup of our experiment; I is the total number of incident particles on the target, which is more convenient to be expressed by the product $Q \times N_0$, where Q is the charge in μCb and N_0 is equal to 6,25 × 10^{12} particles/μCb in

the case of protons; N is the atomic density of target Au, which is equal to $5,9 \times 10^{22}$ at/cm^3 and finally τ is the thickness of Au foil in $\mu gr/cm^2$.
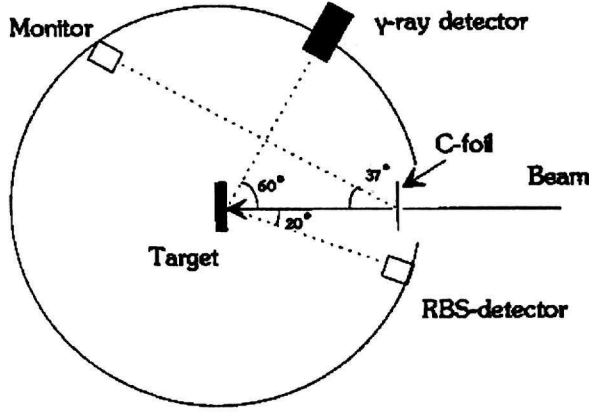

Fig. 1. Experimental setup for profile analysis.

3 Cross section calculation

In order to calculate the cross section for copper and sulfur, we used Eq (1) in reverse. From the yield of the reaction A at an energy E_0 and the corresponding yield $A+\Delta A$ at an energy $E_0+\Delta E$ with the condition $\Delta E \ll E_0$ and providing the cross section changes very slowly with energy in that region, we find after integration and by using the relation $\Delta x = \Delta E/S(E)$, where $S(E)$ is the energy loss in units of $keV \cdot cm^2/\mu g$ for a target of reduced thickness Δx in units of $\mu g/cm^2$, that

$$\sigma(E) = K \frac{\Delta A}{\Delta E} S(E) \qquad (2)$$

where K is a constant. In the case of γ-rays the measured counts are connected with the yield by the relation

$$Y = A \epsilon f w \qquad (3)$$

where ϵ is the detector sensitivity, including the absolute efficiency of the detector and the geometrical solid angle. This parameter depends on the energy of the γ-rays. In the case where we have more than one isotopes of the element in the target, we must multiply with the isotopic abundance f of the reacting

3

isotope, while in the existance of inactive atoms in the target, we multiply with the weight composition w of the active element in the target.

From equations (1),(2) and (3) we finally have for the cross section

$$\sigma = \frac{\Delta Y}{\Delta E} \cdot \frac{B \cdot S(E)}{N_{Av}\, f\, w\, N_0\, Q\, \epsilon} \tag{4}$$

where B is the molecular weight of the target in gr/mole and N_{Av} is the Avogadro number which equals to $6{,}023 \times 10^{23}$ at/mole.

This relation gives the cross section for Cu for the case of non-resonant scattering we mentioned before. However, in the case of S, where we have isolated narrow resonances (all with width $\Gamma \ll \Delta E$), the previous relation is valid only for the non-resonant part of the reaction. For the resonant part, the cross section has the form of Breit-Wigner distribution [6]

$$\sigma(E) = \pi \lambda^2 \omega \frac{\Gamma_i \Gamma_e}{(E - E_R)^2 + (\Gamma/2)^2} \tag{5}$$

where λ is the De-Broglie wavelength, ω the statistical factor, E_R the resonant energy and Γ_i, Γ_e the partial widths for the inelastic and the elastic channel. When the energy width of the target is much greater than the total width of the resonance ($\Delta \gg \Gamma$), that is for the case of a thick target, the quantities λ, Γ_i, Γ_e, $S(E)$, Δ are practically constant in the resonance area and are determined by the value they have at $E = E_R$. So, for thick target measurements, the yield reaches a maximum value $Y_{max}(\infty)$ for $E_0 \gg E_R$, which represents the integral of the resonance over the entire region

$$Y_{max}(\infty) = \frac{\lambda_R^2}{2} \omega \gamma \frac{(M+m)}{M} \frac{1}{S(E)} \tag{6}$$

where M is the mass of the target, m the mass of the projectile and $\gamma = \Gamma_i \Gamma_e / \Gamma$.

In the case where the measurements are taken by a detector placed at an angle θ and subtending a solid angle $\Delta \Omega$, then only a percentage of the total yield of γ-rays is detected, which is given by the relation

$$N(\theta) = Y_{max}(\infty) \frac{N_{Av}}{B} \epsilon f W(\theta) \tag{7}$$

where $W(\theta)$ is the angular distribution of the γ-rays. If there also exist inactive atoms in the target, the energy loss $S(E)$ in Eq (6) must be multiplied by the

4

weigth percentage w of the active element. Finally we have

$$N(\theta) = \frac{\lambda_R^2}{2} w\gamma \frac{(M+m)}{M} \frac{1}{wS(E)} Q\, N^* \,\epsilon\, W(\theta) \frac{N_{Av}}{B} \qquad (8)$$

Furthermore, by integrating Eq (8) over the entire solid angle, the factor $W(\theta)$ is reduced to $4\,\pi A_0$ where A_0 is the coefficient of the zero order Legendre polynomial that enters the angular distribution, so the yield at the specific angle of detection 125° is given by the relation

$$Y(125°) = N(\theta) \frac{2\pi W(125°)}{4\pi A_0} \qquad (9)$$

4   Copper Cross Section

In the case of copper, from Eq (4)·we find the cross section for the non-elastic scattering ^{63}Cu(p,p'γ) for the excitation energy at 1327 keV [7]. The choice of this excitation energy was made so that we have a correspondance with the depth where sulfur resonances are excited. Because of the small number of measured counts, the cross sections calculated with the method we mentioned above have large errors, so when we calculate the yield with the programme PGAMMA (code FORTRAN77) [8], we find deviations from the experimental values. In order to smooth out the cross section, we use a mean value approach whereby to a value of the cross section at a specific energy E we add the cross sections at $E \pm \Delta E$ and take the mean value (for example as the cross section at 3200 keV we take the mean value of the cross sections at 3180, 3200 and 3220 keV). This is not an unreasonable approach, since the cross section for copper does not show any resonant behaviour at the energy region we study, but has a very small, smooth increase with energy. Thus the smoothening procedure gives rise to negligible errors [5]. Furthermore, to the resulting cal- culated yield we add the value of the yield at the lowest energy that we get experimentally (3 MeV), in order to take into account the contribution of the previous values of the cross section of Cu into the excitation function. As a result of the previous procedure we obtain an overall satisfactory agreement between the cross section found by [5] and the cross section that is reproduced by our measurements. So we can use this modified cross section (Fig. 2) in our analysis.

5   Sulfur Cross Section

Eq (9) gives the calculated yield of the reaction ^{32}S(p,p'γ) in the energy region $E \gg E_R$ for CdS, with MB equal to 144,46 g/mole and w equal to 0,222 for
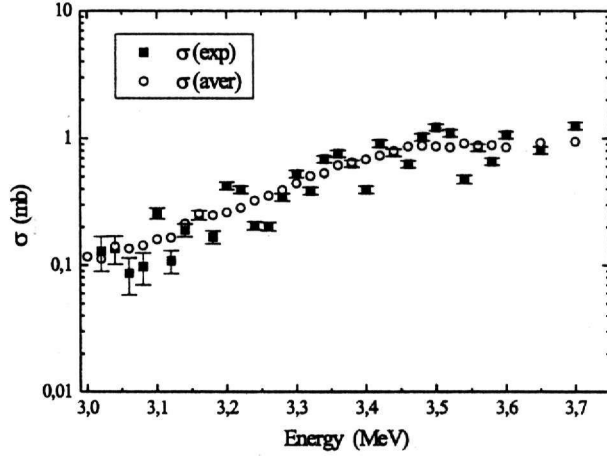
5

Fig. 2. Average experimental and calculated cross section of the reaction $^{63}Cu(p, p'\gamma)$.

CdS; $(M + m)/M$ is equal to 1,032 and $\epsilon(2230 \text{ keV})$ was found $4,26 \times 10^{-4}$. Taking into account the values of $W(\theta)$ and A_0 in the literature [4], we obtain the values shown in Table 1.

Table 1
Values of the resonant parameters λ_R^2, $S(E)$, $W(120°)$ and A_0.

E(keV)	$\lambda_R^2(cm^2)$	$S(E)$ $(keV \cdot cm^2/\mu g)$	$W(120°)$	A_0
3094	$2,73 \times 10^{-24}$	0,05554	0,826	0,9578
3195	$2,65 \times 10^{-24}$	0,05463	2,278	2,0272
3379	$2,50 \times 10^{-24}$	0,05300	1,687	1,5963

From the literature [3,4] and the relations $\gamma = \Gamma_i \Gamma_e / \Gamma$ and $\omega = (2J_1 + 1)/(2s + 1)(2J_0 + 1)$, we find the values for the $\omega\gamma$ of each resonance shown in Table 2. We also represent the resulting yields for the three resonances with their error, together with the experimentally measured yields, which as we can see agree with the calculated values within the error range. The yield units are counts/μ Cb.

From Eq (4) we obtain the values for the cross section. If we assume that apart from the cross section values at 3120, 3220 and 3400 keV (where we observe the highest contribution from the 3 resonances) the rest of the cross section values are non-resonant without significant error, then by inserting them as input to the programme PGAMMA we calculate the yield that comes exclusively from the non-resonant part of the reaction ^{32}S(p,p'γ). If we add

6

Table 2

Width Γ, strength $\omega\gamma$ and yield Y of the three resonances.

E_R (keV)	Γ (keV)	$\omega\gamma$ (keV)	Y_{th}	Y_{exp}
3094	0,34 ± 0,20	0,0605 ± 0,0107	32 ± 7	26,0 ± 3,8
3195	0,44 ± 0,08	0,0098 ± 0,0018	7± 1	6,0 ± 0,3
3379	1,00 ± 0,20	0,320 ± 0,064	206± 40	191 ± 7

to this non-resonant yield the values of the resonant yields that correspond to the three resonances, we obtain the excitation yield of the resonant reaction $^{32}S(p,p'\gamma)$. By comparing this with the experimentally measured, we see very good agreement (figure 5). Also in Table 3 we have the non-resonant cross section for the energy range 3 - 3,7 MeV.
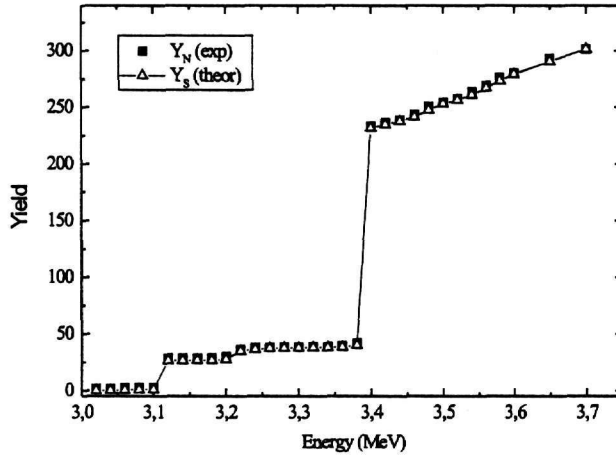

Fig. 3. Excitation function for the reaction $^{32}S(p,p'\gamma)$.

6 Application on patinna samples

Using the cross sections for sulfur and copper which we measured we can now calculate, using the programm PGAMMA the composition of Cu and S with depth for various samples for which we have measured the yield in counts at the peaks at 1327 (for copper) and 2230 keV (for sulfur) respectively. Modifying the composition of S and (or) Cu and the thickness of the various sublayers, we finally obtain a profile of the various ingredients that can reproduce the experimental yield of Cu and S. After this we insert the values

Table 3

Non-resonant cross sections for the reaction $^{32}S(p,p'\gamma)$.

E (MeV)	σ (mb)	$\delta\sigma$ (mb)	E (MeV)	σ (mb)	$\delta\sigma$ (mb)
3,02	0,03977	0,01452	3,36	0,19192	0,01841
3,04	0,02577	0,00898	3,38	1,43950	0,13712
3,06	0,23653	0,06824	3,42	1,53450	0,13520
3,08	0,25029	0,05922	3,44	1,14060	0,10047
3,10	0,01927	0,00412	3,46	2,48350	0,21872
3,14	0,01071	0,00106	3,48	3,42650	0,30158
3,16	0,09512	0,00986	3,50	1,64140	0,14436
3,18	0,02363	0,00245	3,52	1,53000	0,13447
3,20	0,78035	0,07735	3,54	2,92660	0,25698
3,24	0,72974	0,07319	3,56	2,69160	0,23625
3,26	0,14226	0,01417	3,58	3,32270	0,29156
3,28	0,13537	0,01344	3,60	1,78970	0,15692
3,30	0,03131	0,00310	3,65	2,44650	0,21433
3,32	0,15241	0,01505	3,70	1,58110	0,13841
3,34	0,05080	0,00502			

of depth and atomic concentration we have found to the programme RUMP [9], which manipulates the RBS data at 1,5 MeV for the sample. Again we change those values so that we come to an agreement between the experiment and the simulation. After just two iterations between the two simulating programs, we finally obtain a satisfactory aggreement between the calculated and the experimental profile for Cu and S of the specific sample (figures 4 and 5). Thus, in the case of sample CU11, which is made of an antlerite layer on top of a Cu substrate, we obtain the results presented in Tables 4 and 5.

Applying the same techniques, we analysed the samples named as PATINNA COR, 901 and 901 COR. The results are shown in Tables 6-8.

From the values of Table 6 we observe for the sample PATINNA COR that a very thin layer of copper oxide has been formed in the surface, giving rise to much greater numbers to the copper and oxygen composition in that region than expected. This also does not allow us to go deep enough with backscattering spectrometry, since the scattered protons from sulfur are very few and
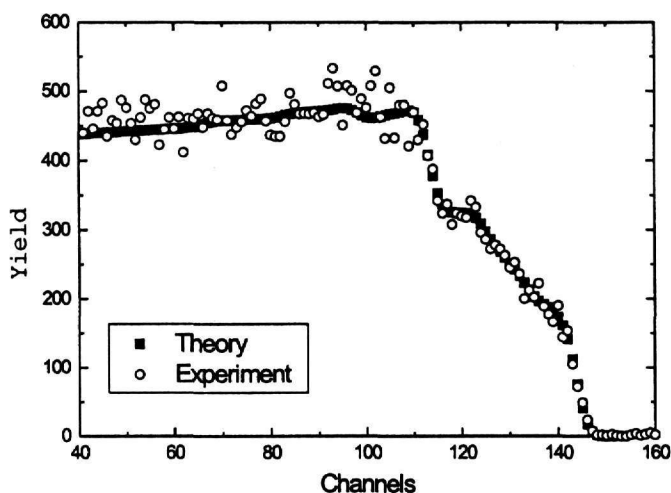
Fig. 4. Backscattering spectrum for the sample CU11.

Table 4
Calculated and experimental yields of S and Cu for the sample CU11.

E(keV)	Calc. S-Yield (counts/μCb)	Exp. S-Yield (counts/μCb)	Calc. Cu-Yield (counts/μCb)	Exp. Cu-Yield (counts/μCb)
3375	11,9	10,9 ± 1,1	18,5	17,2 ± 1,5
3380	12,1	11,3 ± 1,1	19,1	18,0 ± 1,5
3400	66,7	66,7 ± 2,9	21,5	21,3 ± 1,4
3430	74,2	75,4 ± 2,8	25,3	25,3 ± 1,5
3460	78,3	79,3 ± 3,1	29,0	28,0 ± 1,6
3500	74,5	73,7 ± 2,9	34,6	35,9 ± 1,9
3550	70,5	71,9 ± 2,7	41,9	40,1 ± 1,9
3600	84,6	83,5 ± 3,0	48,7	47,8 ± 2,1
3650	79,7	80,1 ± 2,9	54,8	56,7 ± 2,4
3700	77,1	77,7 ± 2,8	60,4	62,4 ± 2,5

the signal they give is covered by the copper background. So we practically see after a certain depth only copper.
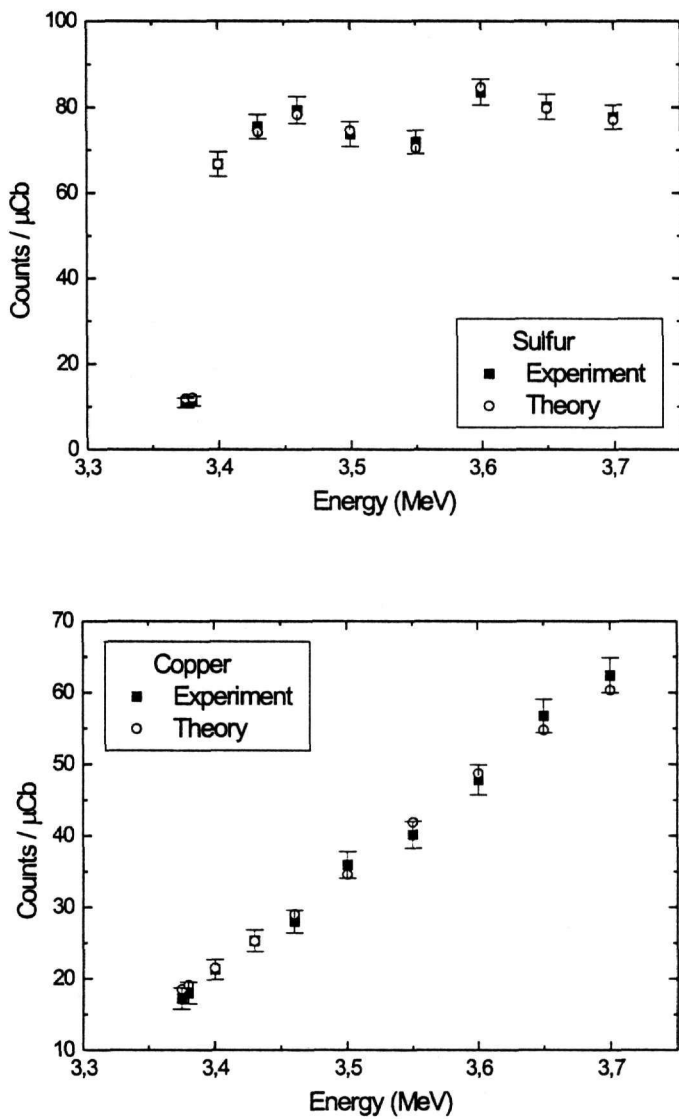
Fig. 5. Experimental yields compared with calculated yields for a) S and b) Cu of sample CU11.

Table 5
Composition of sample CU11.

Sublayer	Atomic ratio				Thickness ($\mu gr/cm^2$)	Total depth ($\mu gr/cm^2$)
	Cu	S	O	H		
1	2,4	1	20	2	140	140
2	2,6	1	17	6	180	320
3	2,8	1	15	6	160	480
4	3,2	1	14	6	150	630
5	3,5	1	12	2	350	980
6	4,5	1	12	2	520	1500
7	5,0	1	11	6	1200	2700
8	4,6	1	8	6	600	3300
9	5,0	1	10	6	600	3900
10	5,4	1	12	6	1600	5500

Table 6
Composition of sample PATINNA COR.

Sublayer	Atomic ratio				Thickness ($\mu gr/cm^2$)	Total depth ($\mu gr/cm^2$)
	Cu	S	O	H		
1	1	0	5	0	60	60
2	9	1	22	8	150	210
3	9	1	11	4	240	450
4	11	1	11	4	240	690
5	11	1	9	4	400	1090
6	15	1	2	2	300	1390
7	5	1	28	10	1300	2690
8	7,5	1	33	10	400	3090
9	9	1	40	10	400	3490
10	12	1	50	15	400	3890
11	15	1	60	15	800	4690
12	5	0	1	0	4000	8690

11

Table 7
Composition of sample 901.

Sublayer	Atomic ratio				Thickness ($\mu gr/cm^2$)	Total depth ($\mu gr/cm^2$)
	Cu	S	O	H		
1	1	0	4	0	70	70
2	5	1	14	2	120	190
3	6	1	11	4	80	270
4	9	1	10	4	140	410
5	9	1	5	4	100	510
6	25	1	13	2	300	810
7	3	0	1	0	280	1090
8	1	0	0	0	650	1740
9	15	0	1	0	1350	3090
10	5	0	1	0	10000	13090

Table 8
Composition of sample 901 COR.

Sublayer	Atomic ratio		Thickness ($\mu gr/cm^2$)	Total depth ($\mu gr/cm^2$)
	Cu	O		
1	1,7	1	300	300
2	2,5	1	270	570
3	3,7	1	510	1080
4	3,3	1	500	1580
5	4	1	370	1950
6	4,8	1	770	2720
7	5	1	850	3570
8	4,2	1	640	4210
9	2	1	2000	6210
10	1	0	20000	26210

7   Conclusions

This work has demonstrated that the combined use of RBS and NRA can lead to a consistent description of inhomogeneous layer structures. This combination takes advantage of the different depth resolution of the two techniques. Samples of widely differing composition can be analysed. It was also demonstrated that finer steps in the NRA measurements are necessary for better resolution. A final point which became apparent is that cross sections of interesting nuclear reactions have to be measured again in more detail with the applications in mind. Most of the data currently available in the literature were obtained for purposes of nuclear spectroscopy. Hence they are either relative or fragmentary.

Acknowledgements

References

[1] V.H. Rotberg, Nucl. Instr. and Meth. 200 (1982) 511.

[2] J. Raisanen and R. Lapatto, Nucl. Instr. and Meth. B 30 (1988) 90.

[3] C. Tsartsarakos, P. Misaelides and A. Katsanos, Nucl. Instr. and Meth. B 45 (1990) 33.

[4] J.W. Olness et al., Phys. Rev. 112 (1958) 1702.

[5] M.E. Sevior et al., Aust. J. Phys. 36 (1983) 463.

[6] C.E. Rolfs and W.S. Rodney, Cauldrons in the Cosmos (The University of Chicago Press, 1988).

[7] R.L. Auble, Nucl. Data Sheets 28 (1979) 559.

[8] G. Kaliambakos, PGAMMA code (1999), unpublished.

[9] L.R. Doolittle, Nucl. Instr. and Meth. B 9 (1985) 344.